Int. j. adv. multidisc. res. stud. 2023; 3(3):390-396

Received: 05-04-2023
Accepted: 15-05-2023

International Journal of Advanced Multidisciplinary Research and Studies

ISSN: 2583-049X

Evaluation of Driving Forces on Wellbore Stability in Shale Formations

Abdul Haque Tunio
University of Engineering & Technology, Jomshoro, Pakistan

Corresponding Author: **Abdul Haque Tunio**

Abstract
Drilling into chemically active shale formations is critical due to the time-dependent interaction between the drilling fluids and the shale. The physical models shown thus far have sophisticated input parameters that necessitate advanced experimental facilities, which are expensive and, in most cases, unavailable. Due to the chemical active shale formation drilling through water base mud is a challenge for petroleum industry. So, in shale formations well instability is a major problem due to the physiochemical interactions of drilling fluids with the formation. In this paper, driving forces i.e., poroelastic, chemical and thermal effects are evaluated for the investigation of dominant driving forces.

Keywords: Driving Forces, Wellbore, Shale Formations, Thermal Diffusion

1. Introduction
During drilling 90% problems arises due to shale as reported by the petroleum industry that costs about one billion dollars per annum (Stephenson MH.2016) [18]. For wellbore instability mechanical, thermal, and chemical effects are the main driving forces. Tensile and collapse are the failure mechanisms (Fjær, Holt *et al.* 2008) [3]. The nature of shale is brittle and ductile type. The ductile nature shows plastic behavior and cause drill string sticking. While brittle nature may cause bridging and well pack-off by failure (Mohammed, H.Q., 2017) [14]. Interaction of water-based drilling fluid with shale cause swelling, as a result of which drill string sticking and hole size reduction occurs (Murtaza, Mobeen, *et al.* 2022) [20]. In shaly formation, excessive pressure of the formation cause well collapse (Ibrahim 2021) [8].The performance of oil based mud is better than water based mud for drilling a shaly formation but are not the best way for drilling such formations because of high drilling costs and environmental issues as reported by some papers (Pacheco 2018) [19].
Shale failure is prime caused by the revamp of in situ stress which eventually excels tensile or shear strength of the rock formation because of which wellbore instability can occur. Therefore, the analysis of wellbore stability includes to achieve the best mud weight window that ensure stability of the well for drilling operations. Hence, the particular mud pressure window should be no more than the fracture gradient and greater than the shear failure gradient (Aslannezhad M, *et al.* 2020) [21] (Agoha, Opara *et al.* 2021) [1]. Additionally, to poroelastic effects, an important factor which affect the wellbore stability is the osmotic pressure. By exposing shale to different fluids (drilling) samples swelling pressure can be observed. With exposure time the shale strength changes as dehydration or hydration progresses (Zeynali, M.E., 2012) [16] (Mkpoikana, Dosunmu *et al.* 2015) [15].
Rock stresses are also affected by thermal diffusion between the formation and the drilling fluid. Thermal impacts, on the other hand, cannot be ignored but are rarely regarded as an alternate method for maintaining wellbore stability, because the rock or the drilling fluid temperature in not easily manageable (Bassey, Akong, *et al.* 2011) [4] (Pandey, Prateek, *et al.* 2013) [5] (Chukwuemeka, Amede *et al.* 2017) [2] (Gao, Yonghai, *et al.* 2019) [12].

2. Theory
2.1 Stress Model
The distribution of local stresses are regulated by in-situ stresses, thermal, chemical and hydraulic effects around the wellbore. For cylindrical hole, the axial, radial and tangential stresses can be determined by generalized Kirsch equation (Aadnøy, Bernt S.2004) [26] (Kanfar 2017) [11] (Thomas, N., & Weijermars, R. 2018) [7].

$$\sigma_{rr} = \frac{1}{2}\left(1 - \frac{r_w^2}{r^2}\right)(\sigma_x + \sigma_y) + \frac{1}{2}\left(1 + 3\frac{r_w^4}{r^4} - 4\frac{r_w^2}{r^2}\right)(\sigma_x - \sigma_y)\cos 2\theta + \tau_{xy}\,(sin2\theta)\left(1 + 3\frac{r_w^4}{r^4} - 4\frac{r_w^2}{r^2}\right) + \frac{r_w}{r^2}Pw$$

$$\sigma_{\theta\theta} = \frac{1}{2}(\sigma_x + \sigma_y)\left(1 + \frac{r_w^2}{r^2}\right) - \frac{1}{2}(\sigma_x - \sigma_y)\left(1 + 3\frac{r_w^4}{r^4}\right)cos\,2\theta - \tau_{xy}\left(1 + 3\frac{r_w^4}{r^4}\right)sin2\theta - \frac{r_w}{r^2}Pw$$

$$\sigma_{zz} = \sigma_z - v\left[2(\sigma_x - \sigma_y)\frac{r_w^2}{r^2}cos\,2\theta + 4\,\tau_{xy}\,\frac{r_w^2}{r^2}sin2\theta\right]$$

$$\tau_{r\theta} = \left[\frac{1}{2}(\sigma_x - \sigma_y)\,sin2\theta\left(1 + 3\frac{r_w^4}{r^4} + 2\frac{r_w^2}{r^2}\right) + \tau_{xy}\,cos\,2\theta\right]\left[\left(1 - 3\frac{r_w^4}{r^4}\right) + 2\frac{r_w^2}{r^2}\right]sin2\theta$$

$$\tau_{\theta z} = (-\tau_{xz}\,sin\theta + \tau_{yz}\,cos\,\theta)\left(1 + \frac{r_w^2}{r^2}\right)$$

$$\tau_{rz} = (-\tau_{xy}\,cos\,\theta + \tau_{yz}\,sin\,\theta)\left(1 - \frac{r_w^2}{r^2}\right)$$

By the help of two derived models by (Lal *et al*. 1999) [13] and (Horsud, P., 2001) [24] UCS can be calculated and make use of sonic logs for finding the above intensity (MUSTAFA 2014) [17]. The models as

$$C_0[MPa] = 0.77\left(\frac{304.8}{\Delta t(sonic)}\right)^{2.93} \quad (2)$$

$$C_0[MPa] = 10\left(\frac{304.8}{\Delta t(sonic)} - 1\right)$$

With time, the cohesive strength also changes as given by (Lal 1999) [13]

$$C = (C_0 - C_e)\exp(at) + C_e$$

Where:

't' = time in days,

Ce = equivalent cohesive strength and

2.2 Induced Stresses

The induced stresses due to hydraulics of fluid flow and temperature are the effective parameters for reflection. For calculation of these induced stresses the following equations are used (Ghassemi, A., and A. Diek.2002) [10] (Ghassemi, Tao *et al*. 2009) [6]

$$\sigma_{rr} = \frac{\alpha_p(1-2v)}{1-v}\cdot\frac{1}{r^2}\int_{r_w}^{r} P_p{}^f(r,t)rdr + \frac{E\alpha_m}{3(1-v)}\frac{1}{r^2}\int_{r_w}^{r} T^f(r,t)rdr \quad (3)$$

$$\sigma_{\theta\theta} = \frac{\alpha_p(1-2v)}{1-v}\cdot\left[\frac{1}{r^2}P_p{}^f(r,t)rdr - P_p{}^f(r,t)\right] - \frac{E\alpha_m}{3(1-v)}\left[\frac{1}{r^2}\int_{r_w}^{r} T^f(r,t)rdr - T^f(r,t)\right]$$

$$\sigma_{zz} = \frac{\alpha_p(1-2v)}{1-v}P_p{}^f(r,t) + \frac{E\alpha_m}{3(1-v)}T^f(r,t)$$

2.3 Pore Pressure

By altering pore pressure, bore hole stability and stress distributions can be affected. Pore pressure profile w.r.t. time and the wellbore radius under initial and boundary conditions are expressed as under (C. Chen 2001) [25].

$$P(r,t) = P_0 + (P_w - P_\pi - P_o)[\text{erfc}\left\{\frac{r-r_w}{2\sqrt{ct}}\right\} - \text{erfc}\left\{\frac{r-r_w}{2\sqrt{c_o t}}\right\}]\sqrt{\frac{r_w}{r}}\,\text{erfc}\left\{\frac{r-r_w}{2\sqrt{ct}}\right\} - \frac{c'(T_w - T_o)}{1 - c/c_o}\sqrt{\frac{r_w}{r}} \quad (4)$$

The initial and boundary conditions are the following.

$P_p(r, 0) = P_i$
$P_p(r_w, t) = P_w$ (5)
$P_p(\infty, 0) = P_i$

For radial system, formation temperature equation is,

$$\frac{\partial T}{\partial t} = C_0\left(\frac{1}{r}\frac{\partial T}{\partial r} + \frac{\partial^2 T}{\partial r^2}\right) \quad (6)$$

The following are the initial and boundary conditions.

$T(r_w, t) = T_w$
$T(r, 0) = T_i$ (7)

$T(\infty, t) = T$

In shale system, osmotic pressure can be determined by equation (8) and can be modified by altering the chemistry of the drilling mud such that the drilling fluid meets the requirements of certain wellbore stability.

$$P_\pi = -I_m \frac{RT}{V} In \frac{a_{wm}}{a_{wsh}} \quad (8)$$

3. Modeling Results

3.1 Input Data

Required data for the analysis of wellbore stability is listed in table 1 (C. Chen, 2001) [25]. These parameters can be measured at the wellhead, laboratory, using appropriate techniques or empirical correlations. All the calculations in this study are dependent upon time and the radial distance of interest is to be 1.3 times the radius of bore hole.

Table 1: Input variables for modelling (C. Chen, 2001) [25]

Parameters	Symbols	Numerical Value	Unit
Geothermal Gradient	G_g	2.00	K/100m
Mud activity	a_{wm}	0.78	unitless
Shale Activity	a_{wsh}	0.9150	unitless
Membrane efficiency	I_m	0.1	unitless
Minimum horizontal in-situ stress gradient	σ_1	0.01877	MPa/m
Overburden gradient	σ_v	0.01945	MPa/m
Mud Gradient	M_w	0.018	MPa/m
maximum horizontal in-situ stress gradient	σ_H	0.01877	MPa/m
Depth (TVD)	D	4352.5	m
Pore pressure Gradient	P_0	0.01538	MPa/m
Wellbore radius	r_w	0.127	M
Well azimuth	A_{zim}	30	Degree
Well inclination	I_w	0	Degree
Biot's parameter	α	0.8	unitless
Drained Poisson's ratio	V	0.22	unitless
Initial cohesive strength	C_φ	8.736	MPa
Tensile strength	σ_1	0.689	MPa
Cohesion alteration factor	a^*	-0.5	unitless
Equilibrium cohesive strength	C_e	5.192	MPa
Failure criteria	-	Drucker Prager	-
Shale Young's modulus	E	6895	MPa
Time	t	0, (8640), (86,400), (864,000)	s
Friction angle	φ	30	Degree
Thermal diffusivity of porous media	C_0	9.50E-14	m^2/s
Pore fluid or mud hydraulic diffusivity	C	3.40E-10	m^2/s
Volumetric thermal expansion coefficient of pore fluid (water)	α_f	5.00E-04	K^{-1}
Coupling coefficient	C_0 ‘	4.25E-14	m^2/s-MPa
Coupling coefficient	C’	1.24E-01	MPa/K
Wellbore wall temperature	T_w	3.51E+02	K
Volumetric thermal expansion coefficient of rock matrix (Shale)	α_m	2.59E-05	K^{-1}
Rock initial temperature	T_o	3.76E+02	K

3.2 Pore Pressure and Collapse Stress

Drucker-Prager Criteria is an additional widely used failure standards which is the expanded form of Von Mises criteria given as (Chen, Guizhong, *et al*. 2003) [22] (Mehranpour MH, Kulatilake PH. 2016) [27]

$$\sqrt{J_2} = AJ_1^{ef} + B \quad (9)$$

Effective Collapse stress = Failure index = FI = $\sigma_{oct} = -\sqrt{J_2} + AJ_1^{ef} + B$ (10)

Where:

$$J_1^{ef} = \frac{\sigma_{rr}+\sigma_{\theta\theta}+\sigma_{zz}}{3} - p(r,t) \quad (11)$$

$$J_2 = \frac{1}{6}((\sigma_{rr}-\sigma_{\theta\theta})^2 + (\sigma_{rr}-\sigma_{zz})^2 + (\sigma_{zz}-\sigma_{\theta\theta})^2) + \sigma_{rz}^2 + \sigma_{r\theta}^2 + \sigma_{\theta z}^2 \quad (12)$$

$$A = \frac{2\sqrt{2}\ \sin\phi}{3-\sin\phi} \quad (13)$$

$$B = \frac{2\sqrt{2}\ c\cos\phi}{3-\sin\phi} \quad (14)$$

When the failure index reaches to negative, failure will occurs (Chen, Guizhong, *et al*. 2003) [22]. Cohesive strength decreases with time to this equivalent cohesive strength, as shown in the Fig 1 as below.

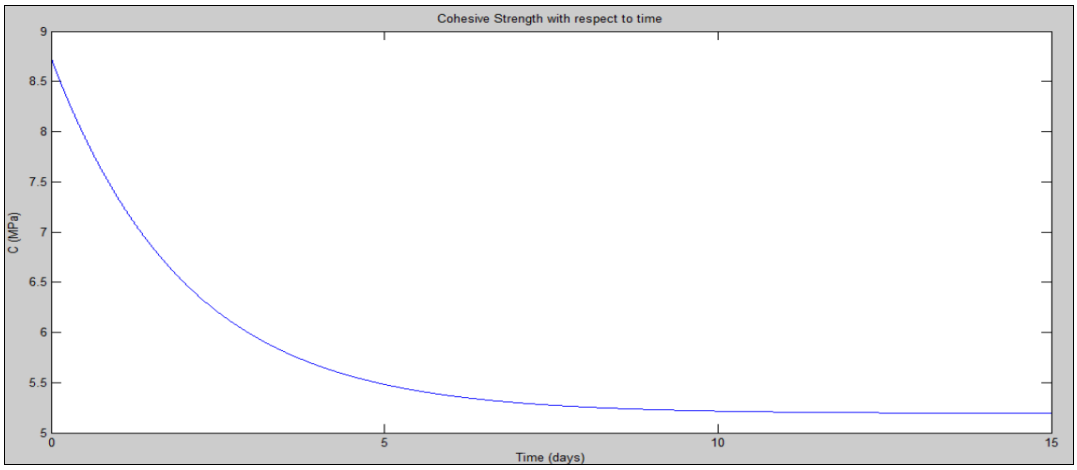

Fig 1: Cohesive strength versus time

When the duration is prolonged, the impacts on the pore pressure can be seen further away from the wall, and the initial pore pressure is not even seen at a specific radius of 1.3 for lengthy times, as in the case when the time was 1 minute. At 1 minute, the effects were only visible near the wellbore wall, and the pore pressure was equal to the original state at any distance away.

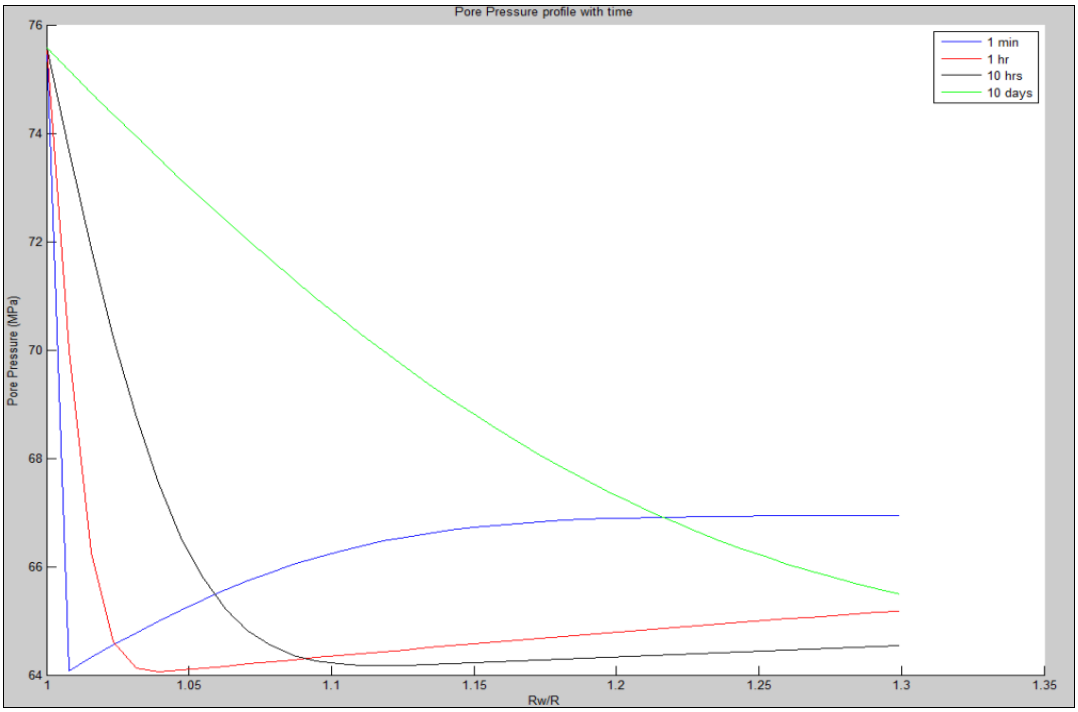

Fig 2: Pore pressure profile at various times

3.3 Chemical Effect

Equation (08) is used for observing the chemical effect**.** When 'R/Rw' is equal to one, then the chemical effects will be applicable only. By moving far away from the wall initial pore pressure goes back to its original value as shown in Fig 3. An effective collapse stress increases due to decrease in pore pressure at the wall as shown in the Fig 4.

Once the effect is not any longer, effective collapse stress graph inclines to keep on the same path as it had exclusive any effects reflected as seen in the Fig 5. Formation activity is higher than the mud activity. Pore pressure reduction occurs because of when the formation fluid is driven out. If the activity in mud had been higher than in the shale formation, a rise in pore pressure is seen near the wall of the wellbore.

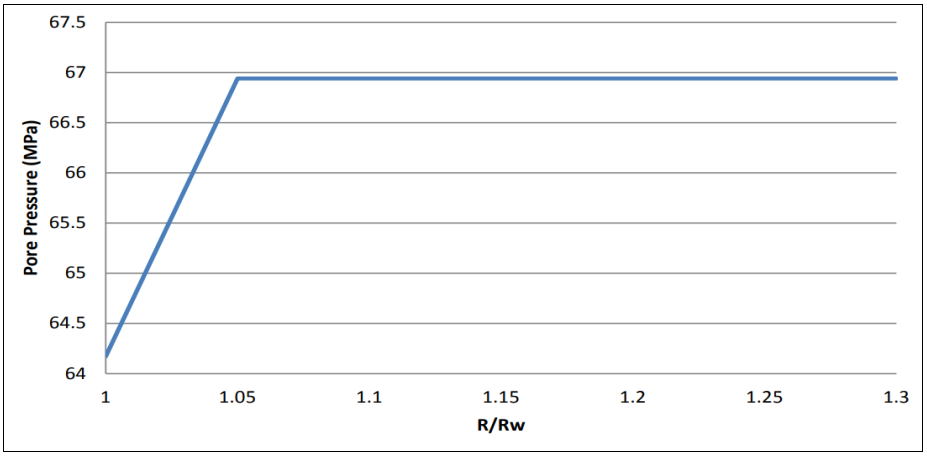

Fig 3: Pore pressure profile for chemical effect

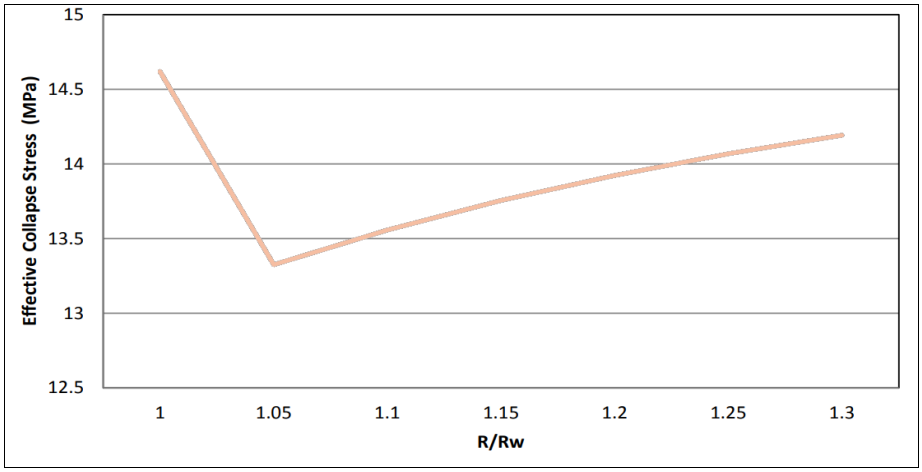

Fig 4: Effective Collapse Stress versus chemical effects

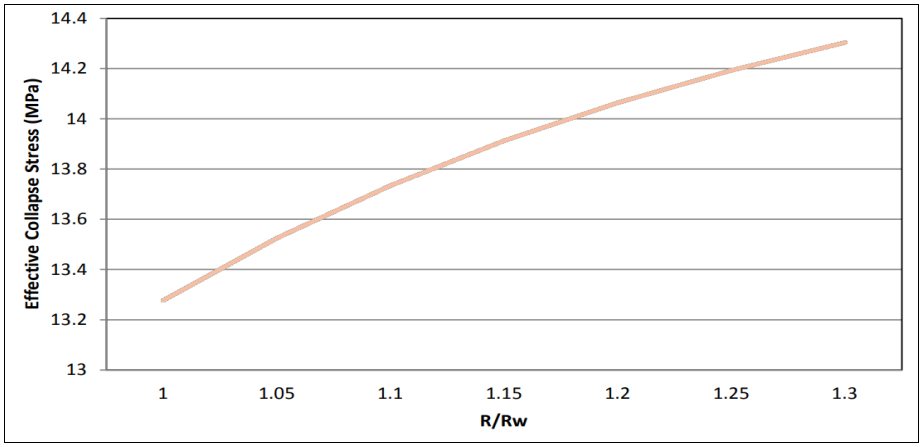

Fig 5: Effective Collapse Stress for no effects

3.4 Thermal effects

For the evaluation of pore pressure profile due to thermal effect equation (04) is used and is shown in Fig 6. Formation temperature is greater than the vicinity of wellbore which outcomes in thermal diffusivity of pore pressure. By moving far away from wellbore, the pore pressure decreases and vice versa. 66.940 MPa pore pressure is all the time at the wall of the wellbore. Till a specific radius of 1.3 some effects can be seen because the pore pressure is not reached its preliminary value highlighting presence of certain thermal effects. In the Fig 7 it is seen that till the specific radius of 1.1 effective collapse pressure increases due to reduction of pore pressure and after that due to small increases in pore pressure the slope of collapse stress occurs till specific radius of 1.3.

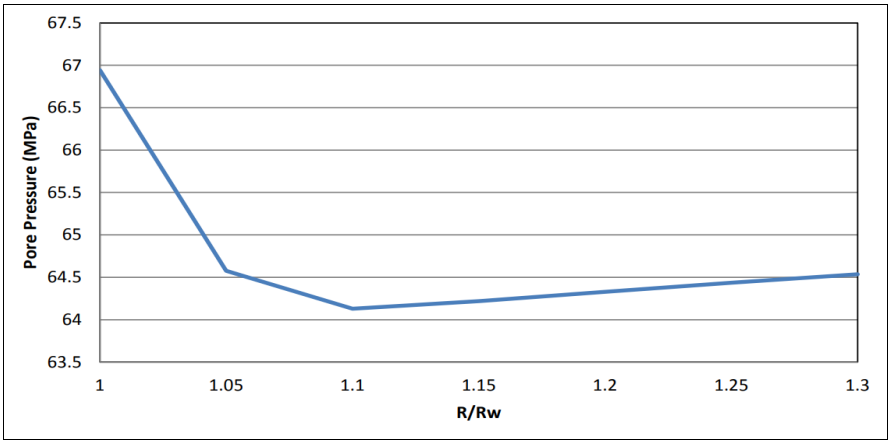

Fig 6: Pore Pressure versus thermal effects

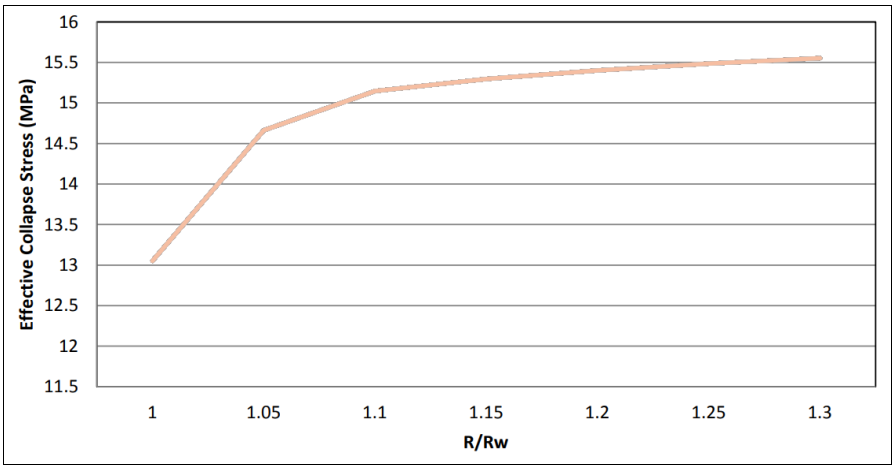

Fig 7: Effective Collapse Stress versus thermal effects

4. Conclusion

1. The permeability of the formation has a significant influence on the stability of the wellbore in shale formation.
2. For compressive failure prevention cooling drilling mud is beneficial.
3. For studying thermal effects in case of wellbore stability the crucial parameter for controlling is expansion coefficient of thermal expansion of rock matrix. There is no significance of thermal effect in such formations having low thermal expansion coefficient.
4. Beside the chemical, mechanical, and thermal effects in low and weak permeable shale formation should be addressed in case of wellbore instability problems.
5. Chemical effect is dominating at the wellbore wall and could be controlled by proper mud design and increase or decrease in pore pressure depends upon the activity of the formation and the drilling fluid.
6. Effective Collapse stress decreases as pore pressure increases and vice versa.

Nomenclature

$\sigma_{rr}, \sigma_{\theta\theta}, \sigma_{zz}$	Radial, Hoop and Axial stress respectively at wellbore
σ_x	Normal stress along x-axis
σ_y	Normal stress along y-axis
r_w	Wellbore radius
r	Near wellbore radial position
$\tau_{r\theta}$	Shear stress at well bore
$\tau_{\theta z}$	Shear stress at well bore
τ_{rz}	Shear stress at well bore
C	Cohesive strength
C_0	Thermal diffusivity
J_2	Shear stress
P_p	Pore pressure
P_o	Initial pore pressure
P_w	Pessure of the Wellbore
P_π	Osmotic pressure
I_m	Efficiency of the membrane
R	Universal gas constant

$P_p{}^f(r,t)$	Pore pressure fluctuations
T_o	Initial formation temperature
$T^f(r,t)$	Temperature fluctuations
I_1^{ef}	Effective mean stress
FI	Failure index
A,B	Material constants

5. References

1. Agoha C, *et al*. Integrated 3D geomechanical characterization of a reservoir: Case study of Fuja field, offshore Niger Delta, Southern Nigeria. Journal of Petroleum Exploration and Production Technology. 2021; 11(10):3637-3662.
2. Chukwuemeka AO, *et al*. A Review of Wellbore Instability During Well Construction: Types, Causes, Prevention and Control. Petroleum & Coal. 2017; 59(5).
3. Fjær E, *et al*. Stability during drilling. Developments in Petroleum Science. 2008; 53:309-339.
4. Bassey, Akong, *et al*. Geomechanical Modelling of Thermal Effects on Wellbore Stability using the Thermo-Poro-Elastic Model in HPHT Wellbores. Nigeria Annual International Conference and Exhibition. OnePetro, 2011.
5. Pandey, Prateek, *et al*. Thermoelectric nanomaterial: a demiurgic approach towards improvement of shale stability. SPE Unconventional Gas Conference and Exhibition. OnePetro, 2013.
6. Ghassemi A, *et al*. Influence of coupled chemo-poro-thermoelastic processes on pore pressure and stress distributions around a wellbore in swelling shale. Journal of Petroleum Science and Engineering. 2009; 67(1-2):57-64.
7. Thomas N, Weijermars R. Comprehensive atlas of stress trajectory patterns and stress magnitudes around cylindrical holes in rock bodies for geoscientific and geotechnical applications. Earth-Science Reviews. 2018; 179:303-371.
8. Ibrahim A. A review of mathematical modelling approaches to tackling wellbore instability in shale formations. Journal of Natural Gas Science and Engineering. 2021; 89:p103870.
9. Chen G, *et al*. Poroelastichemical, and thermal effects on wellbore stability in shales. DC Rocks 2001, the 38th US Symposium on Rock Mechanics (USRMS). OnePetro, 2001.
10. Ghassemi A, Diek A. Porothermoelasticity for swelling shales. Journal of Petroleum Science and Engineering. 2002; 34(1-4):123-135.
11. Kanfar M. Multi-Physics Numerical Modelling of Fluid Flow and Geomechanics for Anisotropic Elasto-Plastic POROUS Media with Applications to Wellbore Stability, UNSW Sydney, 2017.
12. Gao, Yonghai, *et al*. Experimental study on heat transfer in hydrate-bearing reservoirs during drilling processes. Ocean Engineering. 2019; 183:262-269.
13. Lal M. Shale stability: Drilling fluid interaction and shale strength. SPE Asia Pacific Oil and Gas Conference and Exhibition, OnePetro, 1999.
14. Mohammed HQ. Geomechanical analysis of the wellbore instability problems in Nahr Umr Formation southern Iraq. Missouri University of Science and Technology, 2017.
15. Mkpoikana R, *et al*. Prevention of shale instability by optimizing drilling fluid performance. SPE Nigeria Annual International Conference and Exhibition, OnePetro, 2015.
16. Zeynali ME. Mechanical and physico-chemical aspects of wellbore stability during drilling operations. Journal of Petroleum Science and Engineering. 2012; 82:120-124.
17. Mustafa A. Integration Oflith of Acies and Geomechanical Characteristics of Lower Silurian Qusaibashale, Saudiarabia, 2014.
18. Stephenson MH. Shale gas in North America and europe. Energy Science & Engineering. 2016; 4(1):4-13.
19. Pacheco JA. New nanoparticle water-based drilling fluid formulation with enhanced thermal stability and inhibition capabilities in the Woodford shale, Missouri University of Science and Technology, 2018.
20. Murtaza, Mobeen, *et al*. Okra mucilage as environment friendly and non-toxic shale swelling inhibitor in water based drilling fluids. Fuel. 2022; 320:p123868.
21. Aslannezhad M, Keshavarz A, Kalantariasl A. Evaluation of mechanical, chemical, and thermal effects on wellbore stability using different rock failure criteria. Journal of Natural Gas Science and Engineering. 2020; 78:p103276.
22. Chen, Guizhong, *et al*. A study of wellbore stability in shales including poroelastic, chemical, and thermal effects. Journal of Petroleum Science and Engineering. 2003; 38(3-4):167-176.
23. Barrios J, Lobo C, Oroño MV, Campos A. SPE-WVS-394.
24. Horsud P. Estimating Mechanical Properties of Shale from Empirical Correlations, Paper SPE-56017, 2001.
25. Chen C, Chenevert ME, Sharma MM, Yu M. Poroelastic chemical, and thermal effects on wellbore stability in shales. U.S. Symposium on Rock Mechanics. Washington D.C, American Rock Mechanics Association, 2001.
26. Aadnøy, Bernt S, Mesfin Belayneh. Elasto-plastic fracturing model for wellbore stability using non-penetrating fluids. Journal of Petroleum Science and Engineering. 2004; 45(3-4):179-192.
27. Mehranpour MH, Kulatilake PH. Comparison of six major intact rock failure criteria using a particle flow approach under true-triaxial stress condition. Geomechanics and geophysics for geo-energy and geo-resources. 2016; 2:203-229.